Commun Transp Res

Research Article

On-road Evaluation of Emission Control in China V-VI Heavy-duty Diesel Trucks

Weixia Li[1,✉], Ling Miao[1], Guoyuan Wu[2], Wenwei Huang[1], Yi Zhang[3]

Cite this article: https://doi.org/10.26599/COMMTR.2026.9640033

ABSTRACT: This study evaluates the real-world emission impacts associated with the transition from China V to China VI standards for heavy-duty diesel trucks (HDDTs). On-road measurements from 24 HDDTs were obtained using Portable Emission Measurement Systems to quantify particle number (PN) and nitrogen oxides (NOx) emission factors (EFs) under diverse operating conditions. Comparisons were conducted among China V, China VI compliant, and China VI non-compliant vehicles, alongside an assessment of selective catalytic reduction (SCR) and exhaust gas recirculation (EGR) system performance. Fleet-level results indicate that the average PN and NOx EFs of China VI HDDTs were 5.48 and 0.75 times those of China V vehicles, primarily due to a substantial share of non-compliant trucks exceeding regulatory limits. Non-compliant HDDTs exhibited increases of 1,695.6% in PN and 85.6% in NOx EFs relative to China V, whereas compliant vehicles achieved reductions of 51.5% and 59.6%, respectively. Operating mode-specific analysis revealed inadequate PN control at low-to-medium speeds and NOx exceedances under high vehicle-specific power. SCR systems reduced NOx by 76.6-96.8%, with performance varying by compliance and operating mode, while EGR consistently lowered NOx emissions. These findings highlight the necessity for strengthened in-use compliance monitoring and enforcement under China VI regulations.

KEYWORDS: Particle number (PN) emissions; Nitrogen oxides (NOx) emissions; Heavy-duty diesel trucks (HDDTs); China V-VI standard transition; NOx after-treatment systems; Vehicle operating modes

1 Introduction

Heavy-duty diesel trucks (HDDTs) are among the largest contributors to motor vehicle-related air pollutions, particularly with respect to nitrogen oxides (NOx) and particulate matter (PM). According to the China Mobile Source Environmental Management 2025 Annual Report (MEE, 2026), HDDTs accounted for 69.1% of the 4.06 million tons of NOx and 48.5% of the 33 thousand tons of PM emitted by motor vehicles in China in 2024. Similarly, the United States Environmental Protection Agency (USEPA) reported that passenger cars, along with medium-, heavy- and light-duty trucks were the largest sources of transportation-related greenhouse gas emissions (USEPA, 2025). In addition, the transportation sector was responsible for over 55% of NOx emissions and significant quantities of other harmful pollutants including PM and volatile organic compounds (VOCs) in the United States (USEPA, 2023). The California Air Resources Board (CARB) stated that on-road heavy-duty vehicles (HDVs) accounted for more than 30% of total NOx emissions in California (CARB, 2020). The European Road Transport & Emissions Trends Report similarly identified heavy-duty trucks as the second largest contributor of NOx and PM2.5 (PM with an aerodynamic diameter smaller than 2.5 μm) to transportation emissions in the 27 EU Member States (EU27) (EMISIA, 2023). NOx and PM pose serious threats on human health, the environment and the economy. Previous research showed that 3.3% of Beijing residents lived in areas with high HDDT-related PM2.5 exposures, potentially leading to 339 annual premature deaths from non-communicable diseases (NCDs) plus lower respiratory infections (LRIs) (Zhang et al., 2022). In New York city, PM2.5 from vehicle emissions contributed to approximately 320 deaths, and 870 hospitalizations or emergency department visits each year (SEEIC, 2022). According to the European Environment Agency (EEA), exposure to concentrations of PM2.5 and nitrogen dioxide (NO_2) above the 2021 World Health Organization guideline level led to an estimated 238,000 and 49,000 premature deaths in EU27 in 2020 (EEA, 2022). In 2022, 96% and 88% of the EU's urban population remained exposed to annual PM2.5 and NO_2 concentrations exceeding WHO guideline levels of 5 μg/m^3 and 10 μg/m^3, respectively (EEA, 2024).

To reduce emissions from HDDTs, increasingly stringent emission standards have been implemented worldwide. For instance, in the United States, CARB adopted the Advanced Clean Trucks regulation in January 2021 and the Advanced Clean Fleets rule in April 2023 (CARB, 2023). In the European Union (EU), Regulation (EU) 2024/1257 introduced the Euro 7 emission standard, which will apply for new types of HDDTs starting in 2027 (EU, 2024). In China, the Ministry of Ecology and Environment (MEE) issued the latest national emission standard for heavy duty diesel vehicles (HDDVs), titled "Limits and measurement methods for emissions from diesel fuelled heavy-duty vehicles (CHINA VI)" (GB17691-2018), in 2018, which was implemented nationwide in 2021 (MEE and SAMR, 2018). Compared to China V standard, the China VI regulation imposes stricter limits on NOx and particle number (PN) emissions. Specifically, the limits are 400 mg/kWh and 8.0×10^{11} #/kWh for the World Harmonized Steady-state Cycle (WHSC) test, 460 mg/kWh and 6.0×10^{11} #/kWh for the World Harmonized Transient Cycle (WHTC) test, 600 mg/kWh and 16 mg/kWh (PM) for the World Harmonized Not-to-Exceed (WNTE) test,

[1] School of Automotive and Transportation Engineering, Shenzhen Polytechnic University, Shenzhen 518055, China. [2] Bourns College of Engineering - Center for Environmental Research & Technology (CE-CERT), University of California, Riverside CA92507, USA. [3] Department of Automation, Tsinghua University, Beijing 100084, China.

✉ Corresponding author. E-mail: WeixiaLi@szpu.edu.cn

Received: March 26, 2026; Revised: May 8, 2026; Accepted: June 8, 2026

690 mg/kWh and 1.2×10^{12} #/kWh for portable emission measurement system (PEMS) test. Notably, PN control and the PEMS test were introduced for the first time. Additionally, real-time NOx concentration reporting via onboard diagnostics (OBD) became mandatory in the regulation. Numerous studies have demonstrated that stricter emission standards lead to substantial reductions in vehicular emissions (Papadopoulos et al., 2020; He et al., 2020; Shen et al., 2021; Wu et al., 2022; Zhang et al., 2023; Zhao et al., 2024). For example, Papadopoulos et al. (2020) reported reduced real-world NOx and PM emissions from Euro IV to VI medium-duty diesel trucks across different speed bins. Zhang et al. (2023) observed declines in CO_2, CO, NOx and HC emission factors from China III to China IV heavy-duty passenger vehicles. Zhao et al. (2024) found decreased CO_2 and NOx emission factors from China IV to China V container diesel trucks (CDTs) under different vehicle specific power (VSP) bins as well. Accordingly, substantial emission reductions are anticipated under the stricter China VI standard. However, since the implementation of the regulation, most research has focused on evaluating the on-road emission characteristics of China VI HDDTs, such as in-service conformity (ISC) evaluation (Li and Lü, 2021), OBD data-based emission analyses (Wang et al., 2022; Hao et al., 2023; Ge et al., 2023), selective catalytic reduction (SCR) system evaluation (Li et al., 2022), abnormal emission detection (Ge et al., 2023), impacts of after-treatment technologies (He et al., 2024), and emission characteristics under tampered after-treatment systems (Tian et al., 2024). In the authors' previous work (Li et al., 2024), emission characteristics of China VI HDDTs were evaluated with a focus on in-use compliance and intra-standard variability, considering factors such as vehicle features, operating conditions, and the reliability of onboard diagnostic (OBD) NOx data. However, that study was limited to the China VI standard and did not involve inter-standard comparisons. These studies have contributed valuable insights into system-level or individual-vehicle performance but generally lack direct comparative analyses of emission changes across regulatory stages. In addition, most existing studies are limited in sample size and focus on descriptive statistics or individual test cases rather than applying statistical validation to evaluate regulatory impacts at the fleet level. To date, no comprehensive study has quantitatively compared the real-world emission reductions between China V and China VI HDDTs using PEMS, particularly for the newly regulated PN pollutant. The only available comparison relied on OBD-based NOx data (Wang et al., 2022), which does not capture PN emissions. Therefore, the real-world effectiveness of the China VI regulation in reducing both PN and NOx emissions remains insufficiently examined. Given the standard has been in force for several years, a large-scale, PEMS-based comparative evaluation integrating statistical validation, and compliance-based analysis is needed. Such research can provide scientifically grounded evidence for policymakers to assess regulatory performance, guide future emission control strategies, and strengthen in-use conformity frameworks for heavy-duty vehicles.

To address the research gaps outlined above, this research conducted on-road emission tests for both China V and China VI HDDTs to obtain real-world PN and NOx emission data. The regulatory effectiveness of the China VI standard was then evaluated by comparing emissions under various operating conditions. As emission after-treatment systems have been a primary strategy for meeting the stringent emission limits (Ayodhya and Narayanappa, 2018), the real-world performance of the primary NOx control technology of SCR and exhaust gas recirculation (EGR) in China VI HDDTs was also assessed. Finally, potential directions for regulatory improvement were discussed based on the findings. The major contributions of this research are summarized as follows.

- Development of an integrated inter-standard on-road measurement and evaluation methodology. This research proposes and applies a comprehensive methodology for assessing the real-world emission control performance of HDDTs during the China V-VI regulatory transition. In contrast to conventional single-standard or intra-standard analyses, the proposed framework explicitly incorporates inter-standard comparison between China V and China VI vehicles, enabling a systematic evaluation of regulatory effectiveness across emission stages. The methodology combines PEMS-based on-road measurements with both descriptive statistics and statistical validation (e.g., Mann-Whitney U test) under a stratified analytical framework, including overall and in-use compliance differentiated comparisons, operating mode-based emission analysis, and after-treatment performance evaluations.
- First inter-standard comparative PN and NOx assessment for China V-VI transition. This research conducted a structured inter-standard comparison PN and NOx emission comparisons for China V and China VI HDDTs with pollutants measurements form large-scale road tests involving 24 vehicles. Unlike previous studies focusing on emission characteristics within a single regulatory standard, this work directly quantifies the differences in emission behavior across regulatory stages, thereby enabling an evaluation of the real-world effectiveness of the policy transition. To the authors' best knowledge, this is the first research to evaluate the impacts of the China V-VI transition on HDDT emissions, particularly for the newly regulated PN pollutant, and is based on the largest PEMS dataset to date. The results provide quantitative evidence for regulatory authorities to understand the real-world effectiveness of the updated standard, and offer valuable references for other countries to formulate and implement new emission control regulations as well.
- Emission analysis by operating mode and compliance status. The research provided detailed insights through emission comparisons by vehicle operating mode and emission compliance group. HDDTs were categorized into China V, China VI compliant and China VI non-compliant groups based on on-road emission compliance (see Section 2.3.3 for these definitions), and their PN and NOx emissions were analyzed under various operating modes (e.g., idling, braking, low speeds, medium speeds and high speeds). These findings can inform targeted guidance for regulators to strengthen the emission controls and in-use compliance measures.
- Evaluation of SCR effects under different operating conditions. Based on paired upstream-downstream NOx measurements from a subset of vehicles, the analysis provides an empirical evaluation of SCR performance under real-world deployment conditions. This research examined the influence of real-world operating conditions on the NOx control effectiveness of the

SCR systems in China VI HDDTs. By comparing NOx emissions between compliant and non-compliant vehicles and across various operating modes, the study reveals how factors such as driving conditions and exhaust temperature affect the in-use efficiency of SCR systems. These findings provide useful insights for improving emission control strategies and enhancing the real-world performance of after-treatment technologies.

- Assessment of EGR effectiveness in real-world NOx control. This research evaluated the in-use deployment effect of EGR systems based on observational comparisons across vehicles. More specifically, the operating mode-specific impacts of EGR systems on NOx emissions in China VI HDDTs were investigated. By comparing EGR-equipped and unequipped vehicles within both compliant and non-compliant groups, the analysis demonstrated that EGR-equipped vehicles consistently exhibited lower mean NOx emissions across all operating modes, with statistically significant reductions under several medium- and high-speed conditions for compliant HDDTs. The findings confirm the in-use effectiveness of EGR in mitigating NOx emissions and highlight opportunities to further investigate and enhance its performance under low-speed operations.

2 Methodology

To evaluate the effects of emission control policies on HDDTs, real-world emission data from China V and China VI HDDTs were collected using PEMS in large-scale road tests. In this research, China V HDDTs refer to HDDTs newly manufactured, sold or registered between July 1, 2017 and June 30, 2021, when the China V standard was in effect. China VI HDDTs refer to those manufactured, sold or registered after July 1, 2021. For each HDDT, both overall and operating mode-specific emission factors for PN and NOx were calculated, enabling comparative analyses between China V and China VI groups. Additionally, the real-world performance of the SCR system in China VI HDDTs was assessed using upstream and downstream NOx concentrations, and EGR effectiveness was examined by comparing NOx emissions from vehicles with and without EGR. Details on the test vehicles, experimental devices, on-road tests, data processing and calculations are described below.

2.1. Test vehicles and experiment devices

2.1.1 Test vehicles

The test fleet was comprised of 24 HDDTs, including 3 China V HDDTs and 21 China VI HDDTs. The smaller sample size for China V HDDTs was due to the absence of mandatory real driving emission (RDE) testing under the China V standard. Although proposed in the China VI standard in 2018, RDE testing only became mandatory from July 2021 for China VI HDDTs. As a result, only small-scale exploratory RDE tests were conducted in 2019 for China V HDDTs, while large-scale tests were carried out in 2022 for China VI HDDTs after the regulation took effect. The test vehicles covered 8 brands (i.e., Dongfeng, Jiefang, Futian, Chenglong, Haowo, Jianghuai, Shandeka and Shanqi) and 7 engine brands (i.e., Futiankangmingsi, Dachai, Dongfengkangmingsi, Weichai, Xichai, Yuchai and Zhongguozhongqi), representing all top five vehicle brands and seven of the top ten engine brands in the city of Shenzhen, China. Rated engine power ranged from 134 kW to 390 kW. All the China V HDDTs were manufactured in 2019, while most China VI HDDTs were produced in 2021 or 2022, ensuring similar time intervals between manufacture and testing. Vehicle mileage at the time of testing ranged from 5,000 km to 160,000 km. Vehicle curb weight ranged from 5,300 kg to 8,800 kg, with tractive tonnage of 18,000 kg to 40,000 kg. All test vehicles were equipped with exhaust after-treatment systems, including SCR, diesel oxidation catalyst (DOC), and ammonia slip catalysts (ASC). In addition, several vehicles were also fitted with diesel particulate filters (DPF) and exhaust gas recirculation (EGR). Detailed specifications are listed in Table S1 of the supplementary materials.

2.1.2 Emission measurement systems

In this research, NOx and PN emissions were measured using a SEMTCH ECOSTAR (Sensors Inc., 2025a) and a SEMTECH CPN (Sensors Inc., 2025b), two widely-used PEMS (Merkisz et. al., 2017) developed by Sensors, Inc.. The instruments and their installation on the test vehicle are presented in Fig. S1(a), Fig. S1(b) and Fig. S1(c) of the supplementary materials, respectively. The technical specifications are provided in Table S2 and Table S3 of the supplementary materials as well. Instantaneous NO and NO_2 concentrations were recorded at a one-second resolution using the nondispersive ultraviolet (NDUV) module of the SEMTECH ECOSTAR, from which NOx emissions were calculated. PN emissions were recorded at one-second intervals using the SEMTECH CPN. Real-time vehicle operation data (e.g., vehicle speed, engine speed, etc.) were collected via an OBD data logger and used in conjunction with emission rates to calculate EFs (Section 2.3). Additionally, the NOx concentrations from upstream and downstream of the SCR system were also collected via OBD and used to assess the performance of the SCR system (Section 3.3).

2.2. On-road emission tests

2.2.1 Test routes

For on-road emission tests, the Chinese PEMS regulation (MEE and SAMR, 2018) specifies route and procedure requirements for all HDDT subcategories, including N1 (gross vehicle weight (GVW) ≤ 3,500 kg), N2 (3,500 kg < GVW ≤ 12,000 kg) and N3 (GVW > 12,000 kg). All vehicles tested in this research belonged to the N3 category of HDDTs, primarily designed for long-haul freight and heavy-load transport. According to regulatory requirements, the urban, suburban, and freeway operation shares during testing should approximate 20%, 25% and 55%, respectively, with a tolerance of ±5%. In accordance with these requirements, the on-road emission measurements for China V and China VI HDDTs were conducted on the two test routes in Shenzhen.

In both routes, the suburban and freeway operations were performed on the Guangshen Coastal Expressway in southwest Shenzhen. For China V HDDTs, the urban roads included Tongsha Road, Shigu Road, Liuxian Boulevard, Tongle Road, Nanhai Boulevard, North Ring Boulevard and Yueliangwan Boulevard. For China VI HDDTs, the urban roads included Mawaner Road, Xinghai Boulevard and Yueliangwan Boulevard. All the tests began with urban driving at average speeds of 15-30 km/h, followed by suburban segments at 45-70 km/h upon entering the Guangshen Coastal Expressway, and concluded with freeway operations at average speeds above 70 km/h on the same expressway. It is noted that the test routes for the China V and China VI HDDTs were not exactly identical because the on-road measurements were conducted in two separate batches (see Section 2.2.3). During the latter batch of tests, several urban road segments used in the original route were temporarily closed due to construction. To maintain route representativeness and continuity, alternative urban roads were selected to connect with the same suburban and freeway sections as those in the original route. Such minor differences in test routes are permitted under the Chinese PEMS regulation (MEE and SAMR, 2018), which does not require identical routes across vehicles. Instead, the regulation specifies only the shares of urban, suburban, and freeway operations, which were verified during the test data validation step described in Section 2.2.2. Throughout each trip, vehicle activity and emissions were recorded using the measurement systems described in Section 2.1.2.

2.2.2 Test procedures

The test procedures strictly followed the Chinese regulation (MEE and SAMR, 2018). In the first step of measurement systems preparation, linearity verification and calibration of the PEMS gas analyzers were performed using certified calibration gases (zero gas, span gas and gases of known concentrations) in accordance with the specifications outlined in the regulation. The calibration gases used in this research were supplied by Shenzhen Testing Technology Co., Ltd., and included 8 L cylinders of N_2 (100%), 40% H_2 in Helium balance, 12%-13% CO_2, 5000 ppm CO, 2000 ppm NO, 300 ppm C_3H_8 in N_2 balance, and 500 ppm NO_2 in air balance. In the second step of measurement parameter selection, NOx and PN concentrations, exhaust parameters (flow rate and temperature), ambient condition parameters (temperature and barometric pressure), engine parameters (speed, torque, fuel consumption rate, and coolant temperature), vehicle speed, and global positioning system (GPS)-based location data (latitude, longitude, and altitude) were selected as target parameters, as summarized in Table S4. In the third step of test vehicle preparation, each HDDT was loaded with clump weights equivalent to the 50% of its maximum design load. This load selection conforms with the China VI regulation (MEE and SAMR, 2018), which prescribes a test-load range of 50%-100% of maximum design load for Stage 6a and 10%-100% for Stage 6b. In the fourth step of measurement systems installation, PEMS, exhaust flowmeter (EFM), GPS, and electronic control unit (ECU) data logger (i.e., OBD) were installed on the test HDDT. After that, the measurement instruments were powered on, the sampling system was purged, and zero and span points of the gas analyzers were recalibrated. During the test, the HDDT driver maintained speeds within the specified urban (15-30 km/h), suburban (45-70 km/h), and freeway (>70 km/h) ranges along the designed route. After completion, measurement systems verification was conducted to ensure the zero/span drifts were within the required 2% of the full scale. Finally, the test data validation process confirmed that route composition requirements (20%±5% urban, 25%±5% suburban, and 55%±5% freeway) and segment-specific speed ranges (15-30 km/h urban, 45-70 km/h suburban, and >70 km/h freeway) were met. The aforementioned procedures are illustrated in Fig. S2 of the supplementary materials.

2.2.3 Test summary

The on-road tests were conducted in two batches, one for China V HDDTs from September to October in 2019, and the other for China VI HDDTs from October to November in 2022. Summary statistics for each test, including test duration, travel distance, maximum speed and average speed are provided in Table S5. The general features of the measurements include the trajectories of vehicle instantaneous speed as well as NOx and PN emission rates. One China V HDDT (i.e., vehicle #3) and one China VI HDDT (i.e., vehicle #12) are provided as examples in Fig. S3 to aid understanding of the test process. It is noted that the operating conditions of the two HDDTs shown in Fig. S3 exhibit distinct operating patterns, which are mainly attributable to variations in real traffic conditions and driver behavior rather than differences in route design. This interpretation is supported by the additional results presented in Fig. S4 of the supplementary materials, where visible variations in operating conditions are observed even among vehicles tested on the same route. The Chinese PEMS procedure does not require identical driving trajectories as in laboratory-based test cycles but stipulates that the average speeds for urban, suburban, and freeway operation should fall within15-30 km/h, 45-70 km/h, and >70 km/h, respectively, which were verified during the data validation process.

2.3. Data processing and calculations

2.3.1 Vehicle operating modes

To enable a comprehensive comparison of HDDT emissions under varying driving conditions, this study adopted the operating mode binning method. The concept of operating mode was first proposed to represent the operating conditions of light-duty vehicles in the MOtor Vehicle Emission Simulator (MOVES) model in "MOVES2004 Energy and Emission Inputs draft report" (Koupal et al., 2005), and was further extended to heavy-duty vehicles in MOVES2009 (USEPA, 2009). Wu et al. (2012) slightly modified the operating mode bins to better reflect the real-world driving features of HDDVs in China. The modified operating mode bin definitions have been widely applied in the HDDV emission studies in China (e.g., Zheng et. al., 2015, He et. al., 2020) and were adopted in this research as well. To calculate vehicle operating mode, vehicle specific power (VSP), which denotes the instantaneous power demand per unit mass of the vehicle, was first calculated using Eq. (1) (Jiménez-Palacios, 1999), in which, a and v are the instantaneous vehicle acceleration (m/s^2) and speed (m/s), respectively; m stands for the vehicle mass (t); and A, B and C denote the coefficients of rolling resistance (kW·s/m), rotational resistance (kW·s^2/m^2), and aerodynamic drag (kW·s^3/m^3), respectively. These coefficients are derived from a tractive power balance that accounts for the major physical forces acting on a vehicle, including rolling resistance, aerodynamic drag, inertial effects, and road grade, and are determined based on representative vehicle parameters such as mass, drag coefficient, frontal area, rolling resistance coefficient, and air density (Jiménez-Palacios, 1999). In practical applications, these physical parameters are typically grouped into simplified coefficients to facilitate implementation in emission analysis and modeling frameworks such as MOVES (USEPA, 2009). The same $\frac{A}{m}$, $\frac{B}{m}$ and $\frac{C}{m}$ values as in the previous research (Wu et. al., 2012, Zheng et. al., 2015, He et. al., 2020), i.e., 0.0857, 0 and 0.000331, were used in the VSP calculation in this research. These values have been widely adopted in studies of heavy-duty diesel vehicles under real-world driving conditions in China, where vehicle types, loading conditions, and operating environments are comparable, to provide a reasonable approximation of vehicle operating conditions. In addition, as the primary purpose of the VSP calculation in this study is to classify operating modes and enable relative comparisons of emission characteristics across different vehicle groups, the consistent use of the same coefficients for all vehicles ensures internal comparability and minimizes potential systematic bias. θ represents the road grade (in radians). However, as the test routes in the research were relatively flat, the effect of the road grade was negligible.

$$\text{VSP} = av + \frac{A}{m}\cdot v + \frac{B}{m}\cdot v^2 + \frac{C}{m}\cdot v^3 + gvsin\theta \quad (1)$$

With vehicle speeds, accelerations and the calculated VSPs, vehicle instantaneous operating modes were determined according to the definitions in the research of Wu et. al., (2012). A total of 22 operating modes were defined, including a braking (or decelerating) bin, an idling bin, eight low-speed bins, eight medium-speed bins and four high-speed bins. The detailed definitions of the different operating modes are provided in Table S6 of the supplementary materials.

2.3.2 Emission factors

Emission factors (denoted as EFs hereinafter) are widely used in real-world applications, such as regional emission inventory estimations, and are usually expressed as pollutant mass per unit distance. In this research, the overall mean EFs (#/km for PN and g/km for NOx) for each HDDT were calculated from emission rates (denoted as ERs hereinafter) and vehicle speeds using Eq. (2), where ER_t (#/s for PN and g/s for NOx) and v_t (km/h) are the instantaneous emission rate and speed at timestamp t, and T is the maximum timestamp of the test data. A multiplier of 3,600 was applied for unit conversion to g/km. For clarity in subsequent analyses, the NOx EFs were further multiplied by 1,000 to express the results in mg/km.

$$EF_{overall} = \frac{\sum_{t=1}^{T} ER_t}{\sum_{t=1}^{T} v_t} \times 3600 \quad (2)$$

For operating mode-specific EFs, the mean EF calculation equation was presented in (3), where $OpMode_t = i$ indicates that timestamp t belongs to the operating mode of i.

$$EF_{OpMode_i} = \frac{\sum_{OpMode_t=i} ER_t}{\sum_{OpMode_t=i} v_t} \times 3600 \quad (3)$$

2.3.3 Compliant and non-compliant HDDTs

As aforementioned, the emission standard applicable to a HDDT is determined by whether the China V or China VI regulation was in force at the time of its manufacture, sale or registration. All HDDTs must pass the corresponding emission type-approval tests prior to market entry, meaning that China V or China VI HDDTs are essentially vehicles certified to meet the respective regulatory limits. Nevertheless, real-world emissions may deviate from certification values due to factors such as operating conditions, vehicle maintenance, or driver behavior. The China VI regulation introduced PEMS tests into type-approval for the first time, enabling the same method to be applied to in-use vehicles for real-world emission compliance verification. To facilitate a comprehensive comparison with China V HDDTs and assess the effectiveness of the China VI standard, China VI HDDTs in this research were further classified as "compliant" or "non-compliant" according to their real-world emission compliance from PEMS tests. More specifically, vehicle emission compliance was determined using work-based EFs (denoted as EF_w hereinafter), work-based windows and regulatory thresholds. EF_w, expressed as the pollutant mass per unit power (mg/kWh or #/kWh), was calculated from vehicle emission rates and engine power. A work-based window was defined as a continuous time segment in which the accumulated engine work equaled that of a complete transient test cycle (typically the World Harmonized Transient Cycle (WHTC)). The on-road compliance was assessed using the 90th percentile EF_w values across all work-based windows and pollutant concentration limits. Under the China VI standard, the 90th percentile EF_w thresholds for NOx and PN were 690 mg/kWh and 1.2×10^{12} #/kWh, respectively, with an additional requirement that the NOx concentrations remain below 500 ppm for at least 95% of the valid data points. Therefore, a China VI HDDT was determined as NOx-compliant if both the EF_w and concentration criteria were met, and PN-compliant if EF_w threshold was not exceeded. Vehicles failing to meet these criteria were classified as non-compliant. It is noted that only China VI HDDTs were categorized in this way, as China V HDDTs were not subject to PEMS tests or on-road emission thresholds. The detailed methodology has been reported previously (Li et al., 2024) and is not repeated here, as emission compliance results in this research were used solely for vehicle group classification rather than as a primary research objective. In summary, the term "China V" or "China VI" HDDTs refer to certification-based classifications, whereas China VI "compliant" or "non-compliant" HDDTs denote compliance status under real-world operating conditions.

2.4. Statistical analysis methods

To quantitatively evaluate emission differences and relationships among variables, a combination of nonparametric and correlation-based statistical methods was employed, including the Mann-Whitney U (MWU) test, Pearson correlation analysis, and Spearman's rank correlation analysis. These methods were selected based on the characteristics of real-world emission datasets, which typically exhibit non-normal distributions, heteroscedasticity, and the presence of outliers.

The MWU test, originally proposed by Mann and Whitney (1947), is a nonparametric method used to assess whether two independent samples originate from the same distribution. Unlike parametric tests such as the Student's t-test, the MWU test does not require assumptions of normality or equal variances (Fay and Proschan, 2010), making it particularly suitable for environmental and emission data in this research. In this research, the MWU test was applied to compare emission factors between different HDDT groups, including China V, China VI compliant, and China VI non-compliant HDDTs, under both overall and operating mode-specific conditions. The analysis result of the MWU test is presented with p-value, which represents the probability of observing a difference in rank distributions at least as extreme as the one measured, assuming that the null hypothesis of no difference between groups is true. Smaller p-values indicate stronger evidence against the null hypothesis. Differences in p-values across operating modes or vehicle groups reflect variations in both the magnitude and consistency of emission differences under different conditions. For example, a low p-value in a specific operating mode suggests that emission differences between vehicle groups are both large and consistently observed, whereas higher p-values may indicate either smaller differences or greater variability within the data.

It is noted that the sample sizes in this study are unbalanced, comprising 3 China V and 21 China VI HDDTs. Such imbalance, particularly the limited size of the China V group, may reduce statistical power and thereby limit the sensitivity to detect subtle differences between groups. In addition, under small-sample conditions, the discrete nature of the MWU test statistic may result in relatively coarse p-value resolution, and the influence of individual observations in the smaller group may be more pronounced. Nevertheless, the MWU test remains statistically appropriate for comparisons involving unequal sample sizes, provided that observations are independent. To improve the reliability of statistical inference under these conditions, p-values were calculated using exact methods rather than asymptotic approximations. Exact p-values are derived from the exact sampling distribution of the test statistic and do not rely on large-sample assumptions, whereas asymptotic p-values are based on normal approximations that may be less accurate when sample sizes are small or highly imbalanced. The use of exact inference therefore enhances the validity of the statistical results in this study. In addition to hypothesis testing, rank-biserial correlation coefficients are reported as measures of effect size to quantify the magnitude and direction of differences between groups (Kerby, 2014). The rank-biserial correlation reflects the degree of separation between two groups in terms of their rank distributions and can be interpreted as the extent to which values from one group tend to be higher or lower than those from the other group. This provides complementary information to p-values and enables a more comprehensive interpretation of the results. Furthermore, error bar plots (mean ± standard error) are provided to illustrate the relative location and variability of the two groups. These visualizations offer descriptive support for the statistical analysis by showing overall distributional patterns and group separation. In particular, they provide a qualitative indication that the observed differences are not driven solely by extreme observations, but rather reflect general differences in central tendency between groups. The plots further help contextualize the results obtained from the MWU test and corresponding effect size estimates. To ensure the rationality of the findings, the results of the MWU test are interpreted conservatively as well in this study. Given the reduced statistical power associated with the small China V sample, the detection of statistically significant differences indicates that the observed effects are sufficiently pronounced to be identified despite these constraints. As such, statistically significant results in this study provide relatively strong evidence of meaningful differences between groups, rather than marginal or incidental findings. Therefore, statistically significant differences are regarded as robust evidence of differences between groups in this research, while non-significant results are not interpreted as evidence of equivalence but rather as potentially influenced by limited sample size.

To further investigate potential relationships between PN and NOx emissions, Pearson and Spearman's rank correlation analyses were conducted. The Pearson correlation coefficient is used to quantify the strength and direction of linear relationships between continuous variables (Benesty et al., 2009). The coefficient ranges from -1 to +1, where values close to +1 or -1 indicate strong positive or negative linear associations, respectively, and values near zero indicate weak or no linear relationship. The corresponding p-value assesses the statistical significance of the observed correlation under the null hypothesis of no linear association. A small p-value indicates that the observed correlation is unlikely to have occurred by chance, suggesting a statistically significant linear relationship between the variables. Spearman's rank correlation coefficient is a nonparametric measure used to assess monotonic relationships between variables based on their ranked values (Conover, 1999). It is particularly suitable when the relationship may be non-linear or when distributional assumptions are not satisfied. The associated p-value evaluates the significance of the monotonic association under the null hypothesis of no correlation in ranks. A small p-value indicates that the observed association between the ranked variables is statistically significant, implying a consistent increasing or decreasing relationship between the two variables. By combining these two methods, the analysis captures both linear relationships (via Pearson correlation) and more general monotonic relationships (via Spearman correlation), thereby providing a more comprehensive understanding of the associations between PN and NOx emissions.

3 Results and discussions

This section analyzed the emission features of China V and China VI HDDTs both in aggregate and by vehicle operating mode. The primary analytical metrics were descriptive statistics including mean values and standard errors. To assess the statistical significance of EF differences between HDDT groups, the non-parametric Mann-Whitney U test (referred as MWU test hereinafter) was applied. It should be noted that the sample size of China V HDDTs was limited to only three vehicles, which likely reduced the statistical power of the MWU test and contributed to non-significant results in most cases. Nevertheless, the significant findings under certain operating conditions offer valuable insights into the differences in emission features between China V and China VI HDDTs. In addition to comparing the two regulatory categories, the research also evaluated the performance of the SCR and EGR after-treatment system in China VI HDDTs. The NOx reduction performance of the systems was compared across HDDT groups. Statistical analyses using a Pearson correlation and Spearman's rank correlation were also conducted to examine the relationships between SCR NOx reduction effectiveness and vehicle operating modes.

3.1. Overall emission factors of China V and China VI HDDTs

This section provides the quantitative results of the PN and NOx emissions from China V and China VI HDDTs. The mean EFs of PN and NOx from different HDDT groups are illustrated using bar plots with error bars in Fig. 1. Owing to the limited samples, the standard errors could be large. However, comparing the intervals of the sample mean ±1 standard error can still provide a useful reference for interpreting the relative differences between group means. For example, if one interval lies entirely above another, it suggests that the corresponding population mean might be statistically higher. As shown in Fig. 1(a) and 2(c), the mean PN and NOx EFs were 3.67×10^{14} #/km and 497.79 mg/km for China V HDDTs, and 20.1×10^{14} #/km and 373.08 mg/km for China VI HDDTs, respectively. Therefore, China VI HDDTs generally exhibited higher mean PN EF but lower mean NOx EF than China V HDDTs, with mean PN and NOx EFs being approximately 5.48 and 0.75 times of those from China V HDDTs, respectively. The finding of higher PN emissions under the stricter China VI standard is counterintuitive and motivated a further classification of China VI HDDTs into "compliant" and "non-compliant" groups based on real-world emission compliance. Fig. 1(b) and 2(d) show that, as expected, the China VI compliant HDDTs produced lower PN and NOx emissions than China V HDDTs, whereas China VI non-compliant HDDTs exhibited substantially higher emissions of both pollutants. Specifically, the mean PN and NOx EFs were 1.78×10^{14} #/km and 200.99 mg/km for China VI compliant HDDTs, and 65.9×10^{14} #/km and 923.80 mg/km for China VI non-compliant HDDTs. This demonstrates the effective implementation of the China VI standard which ensured HDDTs being emission-compliant could reduce the PN and NOx emissions by 51.5% and 59.6%, respectively, relative to China V HDDTs. Conversely, emissions from China VI non-compliant HDDTs increased by 1,695.6% for PN and 85.6% for NOx. The *p*-values of the

MWU test for PN EFs comparing China V vs. China VI HDDTs, China V vs. compliant China VI HDDTs, and China V vs. non-compliant China VI HDDTs were 0.23, 0.50, and 0.048, respectively. The corresponding p-values for NOx EFs were 0.45, 0.17, and 0.39, respectively, as summarized in Table S7 of the supplementary materials. Notably, despite the small sample size for China V HDDTs (n=3), a statistically significant difference in PN EFs between China V HDDTs and China VI non-compliant HDDTs was still observed.

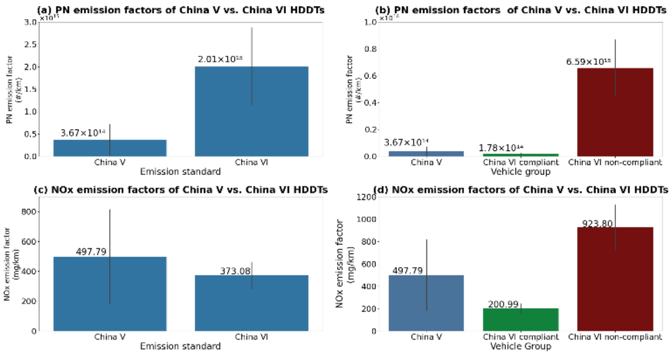

Fig. 1. Emission factors of different vehicle groups

3.2 Comparative emission results by operating modes

This section provides a detailed analysis of HDDT emission characteristics across different operating modes. Emissions from China V and China VI HDDTs, further separated into China VI compliant and non-compliant HDDTs, were calculated and compared across operating modes, with stratification by vehicle speed and VSP levels.

3.2.1 Results for operating mode-specific PN emissions

The PN EFs for different vehicle groups are depicted in Fig. 2, with zoomed-in subfigures for low- and medium-speed modes to improve visual contrast, as the PN EFs from China VI non-compliant vehicles were one to two orders of magnitude higher than those from China VI compliant and China V vehicles. The idling mode was excluded from EF analysis in Fig. 2 due to the zero-distance divisor, instead, the metric of mean emission rate (ER) is reported below. Several mode bins (i.e., 11, 17, 18 and 21) were excluded due to the small sample sizes (less than 10 for most vehicles) in the operating mode-specific EFs. In idling mode, the mean ERs for China V, China VI, China VI compliant and China VI non-compliant HDDTs were 5.73×10^{11} #/s, 4.23×10^{11} #/s, 2.79×10^{11} #/s and 7.85×10^{11} #/s, respectively. Detailed EF and ER values in all operating modes are provided in Table S8 of the supplementary materials. The results show that the overall PN emissions from China VI HDDTs in mean ER were 26.2% lower than those from China V HDDTs in idling mode with reductions of 51.4% for compliant HDDTs but an increase of 37.0% for the non-compliant HDDTs. In braking mode, China VI HDDTs exhibited 64.4% higher PN EFs than China V HDDTs. Within this category, the compliant vehicles showed 73.4% lower PN EFs, while the non-compliant vehicles showed a 409.8% increase relative to China V HDDTs. In low-, medium- and high- speed mode-, similar trends as in braking mode could be found in Fig. 2(a), i.e., China VI HDDTs generally had higher PN EFs than China V HDDTs, largely driven by the non-compliant group, as depicted in Fig. 2(b). Notably, even China VI compliant HDDTs often emitted more PN than China V HDDTs in the operating modes of low-to-medium speed with high VSPs (e.g., bin 15, 16, 23, 24, 25, 27 and 28), with increases ranging from 12.6% to 1,187.6%. In high-speed bins, China VI HDDTs generally exhibited higher PN EFs (30.5-346.6%) except for bin 36. In these high-speed modes, the compliant achieved PN reductions of 49.1-86.4%.

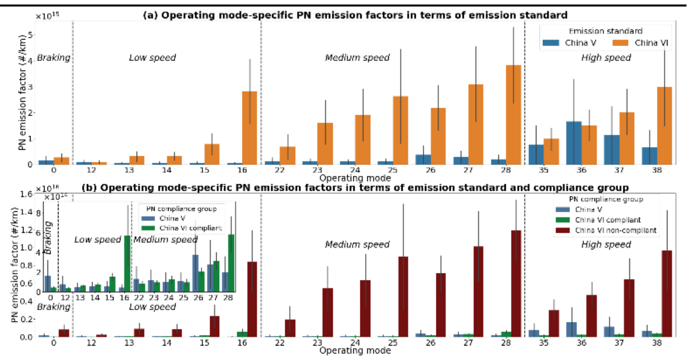

Fig. 2. Operating mode-specific PN EFs from different vehicle groups

The results of the MWU tests, including *p*-values for statistical significance and rank-biserial correlations for effect size, for PN EFs from 3 China V HDDTs, 15 China VI compliant HDDTs, and 6 China VI non-compliant HDDTs, are presented in Table 1. The superscript letter a for operating mode 1 denotes that ERs were used for statistical analysis, whereas EFs were used for the other operating modes. It confirmed that the PN EFs of China V HDDTs and China VI non-compliant HDDTs were significantly different (highlighted with superscript * in Table 1) for half of the evaluated operating modes, particularly in medium-speed bins, with China VI non-compliant HDDTs consistently producing higher PN emissions.

Table 1. MWU test results for operating mode-specific PN EFs

Operating Mode	*p*-value (rank-biserial correlation)		
	China V vs. China VI	China V vs. China VI compliant	China V vs. China VI non-compliant
0	0.310 (0.40)	0.426 (0.33)	0.262 (0.56)
1[a]	0.451 (0.30)	0.574 (0.24)	0.381 (0.44)
12	0.354 (0.37)	0.426 (0.33)	0.381 (0.44)
13	0.234 (0.46)	0.360 (0.38)	0.167 (0.67)
14	0.234 (0.46)	0.426 (0.33)	0.095 (0.78)
15	0.066 (0.68)	0.130 (0.60)	0.048* (0.89)
16	0.011* (0.87)	0.027* (0.82)	0.024* (1)
22	0.356 (0.37)	0.611 (0.23)	0.167 (0.67)
23	0.202 (0.49)	0.426 (0.33)	0.048* (0.89)
24	0.202 (0.49)	0.426 (0.33)	0.048* (0.89)
25	0.234 (0.46)	0.574 (0.24)	0.024* (1)
26	0.271 (0.43)	0.574 (0.24)	0.048* (0.89)
27	0.202 (0.49)	0.426 (0.33)	0.048* (0.89)
28	0.066 (0.68)	0.130 (0.6)	0.048* (0.89)
35	0.452 (0.30)	0.738 (0.16)	0.167 (0.67)
36	0.310 (0.40)	0.498 (0.29)	0.167 (0.67)
37	0.310 (0.40)	0.498 (0.29)	0.167 (0.67)
38	0.234 (0.46)	0.498 (0.29)	0.048* (0.89)

Note: applicable to all subsequent tables: * denotes statistically significant results; superscript a denotes emission rate (ER) values used for the idling operating mode.

In summary, 1) the real-world implementation of the China VI standard did not consistently reduce PN emissions at the fleet level, as a substantial fraction (28.6%) of the China VI HDDTs were PN emission non-compliant, exhibiting significantly higher PN emissions than China V HDDTs. Although the descriptive statistics indicate that China VI compliant HDDTs produced lower mean PN EFs than China V HDDTs under some operating modes, these reductions were not statistically significant with the available sample size (likely due to limited test power). In contrast, the PN EFs of China VI non-compliant HDDTs were significantly higher than those of China V HDDTs, as confirmed by the MWU test; 2) Even among the PN emission compliant China VI HDDTs, the mean PN EF reductions were mainly observed in high speed operating modes, with limited or negative benefits in low-to-medium speed modes under high VSPs (denoting operating conditions with large accelerations in the specific speed levels). Since the China V standard regulated PM mass rather than PN, and PN limits were newly introduced in China VI, further technical and regulatory measures are needed to target PN reductions, especially in low-to-medium speed operations with high-VSPs. Additionally, investigating the mechanisms underlying the PN reduction disparities across operating modes will also be essential for improving compliance and emission control effectiveness.

3.2.2 Results for operating mode-specific NOx emissions

The comparative results of NOx EFs for China V, China VI, China VI compliant and China VI non-compliant HDDTs are presented in Fig. 3.

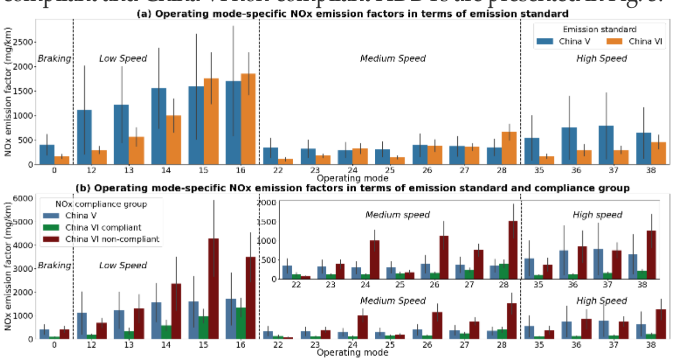

Fig. 3. Operating mode-specific NOx EFs from different vehicle groups

For visual clarity, the results for medium-to-high speed modes are enlarged in Fig. 3(b). The NOx ERs of the four vehicle groups during idling were 2.04 mg/s, 1.15 mg/s, 0.69 mg/s, and 2.64 mg/s, respectively. Detailed EF and ER values for all operating modes are provided in Table S9 of the supplementary materials. In idling mode, China VI HDDTs exhibited a 43.6% reduction in NOx EFs compared with China V HDDTs, in which compliant vehicles achieved a 66.2% reduction, whereas non-compliant vehicles emitted 29.4% more NOx. A similar pattern was observed in the braking mode, where the NOx EFs for the China VI, China VI compliant, and China VI non-compliant HDDTs were 60.1% lower, 78.8% lower and 0.03% higher, respectively, than China V HDDTs. In contrast to PN emissions, where China VI HDDTs produced higher values in most operating modes, the NOx EFs for China VI HDDTs were lower in most operating modes, except for bin 15, 16, 24 and 28, which are characterized by relatively high VSP values (Fig. 3(a)). In the majority bins, NOx EF reductions ranged from 1.8% to 73.5%, In the exception bins, the NOx EFs increased by 8.4-89.3%, in which the higher NOx EFs were mainly attributed to the non-compliant vehicles, since the compliant vehicles only exhibited higher (13.3%) NOx EFs in bin 28, and lower (21.4-61.2%) NOx EFs in the other three bins (Fig. 3(b)). Further stratification by vehicle emission compliance groups revealed that China VI non-compliant HDDTs produced higher NOx EFs in most operating modes, with increases of 6.2% to 332.4%, except for bin 12, 22, 25, 35 and 37, where reductions of 4.4% to 78.3% were observed. The largest increases occurred in high VSP bins, such as bin 15, 16, 26, 27, 28 and 38, where NOx EFs rose by 95.2-332.4%. On the contrary, China VI compliant HDDTs produced less NOx emissions than China V HDDTs in most operating modes (except for bin 28), with reductions ranging from 21.4% to 84.6%. The statistical test results for NOx EFs between HDDT groups were presented in Table 2. As shown in the table, although substantial differences in emission values were observed among the tested vehicles, statistically significant differences were detected in only a few operating modes due to the limited sample sizes (3 China V HDDTs, 16 China VI compliant HDDTs, and 5 China VI non-compliant HDDTs).

Table 2. MWU test results for operating mode-specific NOx EFs

Operating Mode	***p*-value (rank-biserial correlation)**		
	China V vs. China VI	**China V vs. China VI compliant**	**China V vs. China VI non-compliant**
0	0.052 (-0.71)	0.008* (-0.92)	1 (-0.07)
1[a]	0.202 (-0.49)	0.138 (-0.58)	0.786 (-0.2)
12	0.202 (-0.49)	0.085 (-0.67)	1 (0.07)
13	0.145 (-0.56)	0.047* (-0.75)	1 (0.07)
14	0.202 (-0.49)	0.085 (-0.67)	1 (0.07)
15	0.935 (-0.05)	0.634 (-0.21)	0.393 (0.47)
16	1 (0.02)	0.793 (-0.13)	0.393 (0.47)
22	0.021* (-0.82)	0.047* (-0.76)	0.036* (-1)
23	0.202 (-0.49)	0.064 (-0.71)	0.786 (0.2)
24	0.354 (-0.37)	0.064 (-0.71)	0.143 (0.73)
25	0.101 (-0.62)	0.064 (-0.71)	0.571 (-0.33)
26	0.505 (-0.27)	0.171 (-0.54)	0.25 (0.6)
27	0.561 (-0.24)	0.211 (-0.5)	0.25 (0.6)
28	0.935 (0.05)	0.634 (-0.21)	0.071 (0.87)
35	0.680 (-0.17)	0.487 (-0.29)	0.786 (0.2)
36	0.805 (-0.11)	0.487 (-0.29)	0.393 (0.47)
37	0.620 (-0.21)	0.359 (-0.38)	0.571 (0.33)
38	0.680 (-0.17)	0.359 (-0.38)	0.393 (0.47)

In summary, according to the descriptive statistics, 1) the real-world implementation of the China VI emission standard can effectively reduce HDDT NOx emissions in most operating modes, even though 23.8% of the test vehicles failed to meet the NOx limits; 2) substantial NOx reductions are achievable when HDDTs comply with China VI NOx emission requirements; 3) China VI non-compliant HDDTs generated much higher NOx emissions under high VSP conditions (indicative of high power demand due to rapid accelerations at specific speeds), which should be a priority for future regulatory control.

3.3. SCR effects on NOx emissions under different operating conditions

This section analyzes the in-use NOx control effectiveness of the SCR after-treatment system installed in China VI HDDTs. All the 21 China VI HDDTs were equipped with SCR systems. For 12 of these vehicles (i.e., vehicle #5, #6, #7, #8, #9, #11, #14, #15, #20, #21, #23 and #24), both upstream and downstream NOx concentrations were recorded via OBD. These paired measurements were used to determine the NOx reduction efficiency of the SCR systems and to compare the operating-condition-dependent performance between emission-compliant and non-compliant vehicles. Although upstream–downstream measurements were not available for all vehicles, the sample of 12 vehicles is considered sufficient to capture representative trends in SCR performance under real-world conditions. The use of paired measurements within the same vehicle enables a direct evaluation of SCR conversion efficiency while minimizing the influence of between-vehicle variability. Therefore, the results are interpreted as an empirical assessment of SCR in-use effectiveness rather than a fully controlled causal analysis.

Fig. 4 presents the SCR effects across different operating modes, showing the upstream and downstream NOx concentrations, the percentage reductions of NOx concentrations, and comparisons between compliant and non-compliant vehicles. The statistical results of the MWU test are summarized in Table 3. Detailed EF and ER values for all operating modes are provided in Table S10 of the supplementary materials. As shown in Fig. 4(a) and Table 3, the downstream NOx concentrations were significantly lower than the upstream values, confirming the critical role of the SCR system in reducing tailpipe NOx emissions. As depicted in Fig. 4(b), the NOx reduction efficiencies ranged from 76.6% to 96.8%, with generally lower values observed under low-speed operating modes. This result helped explain the relatively higher NOx EFs observed in low-speed modes (see Fig. 3). Comparisons between compliant and non-compliant China VI HDDTs (Fig. 4(c) and Table 3) show that the compliant vehicles achieved consistently higher NOx reductions in most operating modes (except for bin 16 and 22), with differences ranging from 0.9% to 11.5%. The MWU test results in Table 3 confirmed that these reduction differences between the 7 compliant HDDTs and the 5 non-compliant HDDTs were statistically significant under high-speed operating modes, suggesting that improving SCR efficiencies under high-speed conditions for non-compliant vehicle could be an effective emissions-reduction strategy.

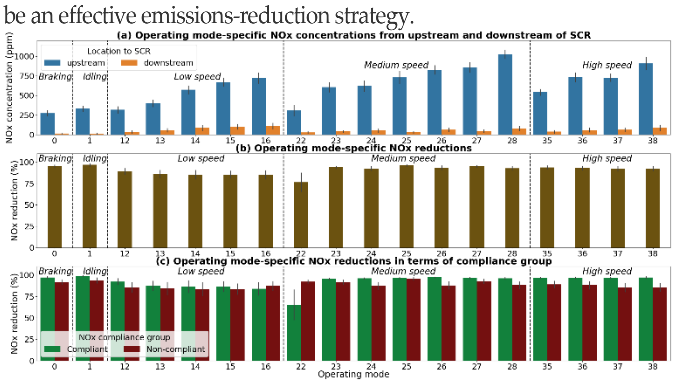

Fig. 4. Effects of SCR system under various operating modes

Table 3. The MWU test results for the upstream and downstream NOx concentrations

Operating Mode	***p*-value (rank-biserial correlation)**	
	upstream vs. downstream NOx concentrations	**NOx reductions of compliant vs. non-compliant HDDTs**
0	$3.7\times10^{-5*}$ (-1)	0.07 (-0.66)
1	$3.7\times10^{-5*}$ (-1)	0.03^{*} (-0.77)
12	$1.2\times10^{-4*}$ (-0.93)	0.15 (-0.54)
13	$4.7\times10^{-5*}$ (-0.99)	0.76 (-0.14)
14	$4.7\times10^{-5*}$ (-0.99)	0.64 (-0.2)
15	$3.7\times10^{-5*}$ (-1)	0.43 (-0.31)
16	$4.7\times10^{-5*}$ (-0.99)	1.0 (0.03)
22	0.01^{*} (-0.63)	0.87 (0.09)
23	$3.7\times10^{-5*}$ (-1)	0.15 (-0.54)
24	$3.7\times10^{-5*}$ (-1)	0.20 (-0.49)
25	$3.7\times10^{-5*}$ (-1)	1.0 (-0.03)
26	$3.7\times10^{-5*}$ (-1)	0.03^{*} (-0.77)
27	$3.7\times10^{-5*}$ (-1)	0.20 (-0.49)
28	$3.7\times10^{-5*}$ (-1)	0.03^{*} (-0.77)
35	$3.7\times10^{-5*}$ (-1)	0.03^{*} (-0.77)
36	$3.7\times10^{-5*}$ (-1)	0.03^{*} (-0.77)
37	$3.7\times10^{-5*}$ (-1)	0.02^{*} (-0.83)
38	$3.7\times10^{-5*}$ (-1)	0.01^{*} (-0.89)

In addition to the MWU test for testing potential group differences, Pearson and Spearman correlation analyses were also conducted to evaluate potential linear or monotonic relationships, and the statistical results are provided in Table S11 of the supplementary materials. Results show that the NOx reductions for compliant China VI HDDTs were linearly and monotonically positively correlated with operating mode with *p*-values of 0.006 and 0.002 from Pearson correlation test and Spearman' s rank test, while no significant correlations were found for the non-compliant HDDTs with corresponding *p*-values of 0.44 and 0.82. The absence of correlation in the latter group might be linked to their relatively low NOx reductions at high speeds. Given that SCR efficacy was affected by exhaust temperature (Tan et al., 2019), the relationship between the operating mode and the exhaust temperature was further examined. A Pearson's correlation coefficient of 0.50 with a *p*-value of 4.6×10^{-15} was found between the operating mode and the exhaust temperature, demonstrating the moderate positive linear relationship, and a Spearman's rank test yielded the *p*-value of 2.2×10^{-22}, indicating a strong monotonic relationship between the two variables. The mean exhaust temperatures across operating modes are shown in Fig. S5 of the supplementary materials. It is noted that the mean exhaust temperatures shown in Fig. S5 are lower than those typically reported in SCR-related studies (Tan et al., 2019), as the data presented here represent tailpipe exhaust temperatures rather than engine-out or SCR-inlet measurements. The lower values are attributed to thermal losses along the exhaust system. Since these temperature data was used solely for exploring correlations with operating mode rather than for quantifying SCR efficiency, the use of downstream tailpipe exhaust temperature is considered appropriate for comparative analysis. The lower exhaust temperature under low speed operating modes likely contributed to the reduced SCR performance due to incomplete urea decomposition and decreased catalyst activity. Therefore, enhancing SCR functions in low-speed modes is also a promising avenue for further NOx reductions in HDDTs.

3.4. EGR effects on NOx emissions under different operating conditions

In this section, the potential impacts of the EGR systems on NOx control effectiveness in China VI HDDTs were investigated. Among the 21 China VI test vehicles, 11 (i.e., vehicle #4, #7, #8, #10, #11, #15, #18, #19, #21, #23 and #24), were equipped with EGR systems. Unlike the SCR effect analysis, where both upstream and downstream NOx concentration were available from the OBD interface, the NOx data from upstream and downstream of the EGR system were not recorded. Therefore, the influence of EGR was assessed by comparing the NOx EFs between EGR-equipped and EGR-unequipped vehicles. This approach represents an observational comparison across vehicles and does not isolate the EGR effect from other influencing factors such as engine calibration, after-treatment strategies, or operating conditions. Accordingly, the analysis is intended to evaluate the real-world deployment effect of EGR systems rather than to establish direct causal relationships. To minimize potential bias due to overall emission compliance, the comparisons were also performed separately for subgroups of compliant and non-compliant HDDTs. The sample sizes were 9, 7, 2, and 3 for the groups of EGR-equipped and compliant, EGR-unequipped and compliant, EGR-equipped and non-compliant, EGR-unequipped and non-compliant, respectively. The descriptive statistics of the mean NOx EFs with standard errors from different groups are illustrated in Fig. 5. Given the relatively small sample sizes in certain subgroups, particularly for non-compliant vehicles, the results are interpreted with caution and primarily used to identify consistent trends in emission behavior under real-world conditions.

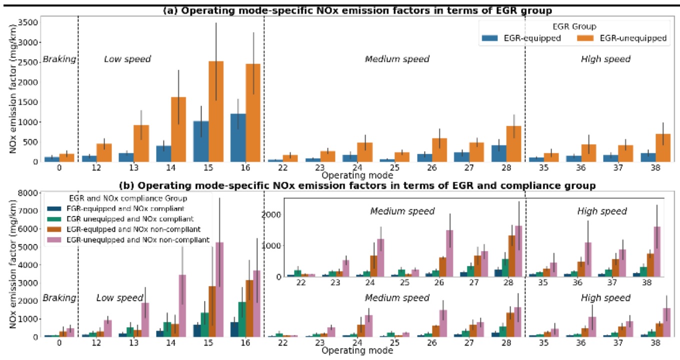

Fig. 5. Operating mode-specific NOx EFs from different EGR groups

Fig. 5(a) presents the NOx EFs of EGR-equipped and EGR-unequipped HDDTs across different operating modes (excluding idling), while Fig. 5(b) compares NOx EFs for compliant and non-compliant vehicles with or without EGR systems. Under the idling mode, the mean NOx ERs were 0.55 mg/s and 1.80 mg/s for the EGR-equipped and EGR-unequipped HDDTs, respectively. For the four subgroups, i.e., EGR-equipped and NOx-compliant, EGR-unequipped and NOx-compliant, EGR-equipped and NOx-noncompliant, and EGR-unequipped and NOx-noncompliant, the mean NOx ERs were 0.58 mg/s, 0.80 mg/s, 0.40 mg/s, and 4.14 mg/s, respectively. Detailed EF/ER values for all operating modes are provided in Table S12 of the supplementary materials.

The results in Fig. 5 and Table S12 demonstrate that EGR-equipped vehicles emitted lower NOx than those without EGR across all operating modes, consistent with the NOx reduction effect under the WHTC tests described by Deng et al. (2025). The NOx reductions were 69.4% in idling and 43.5% in braking modes, and ranged from 51.3% to 75.7% across other operating modes. Similar reduction trends were observed within both compliant and non-compliant subgroups. Specifically, for compliant HDDTs, NOx reductions were 27.0%, 17.6%, and 41.7%~76.7% under idling, braking, and other operating modes, respectively. For non-compliant HDDTs, the corresponding reductions were 90.3%, 33.4%, and -1.6%~80.6%. To assess whether the observed differences were statistically significant, the MWU test was applied to the compliant HDDT group (the non-compliant group was excluded due to its small sample size of 2 and 3 vehicles). The resulting *p*-values are summarized in Table 4. The MWU test confirmed that EGR-equipped compliant HDDTs exhibited significantly lower NOx emissions than those without EGR under several operating modes (i.e., mode 0, 1, 23, 24, 25, 36, 37), demonstrating the in-use effectiveness of EGR in reducing NOx emissions during medium- to high-speed operations, while also indicating the potential need to further improve its performance under low-speed conditions.

Table 4. The MWU test results for NOx EFs between EGR-equipped and unequipped compliant HDDTs

Operating Mode	*p*-value (rank-biserial correlation)
0	0.007* (0.78)
1ᵃ	0.02* (0.68)
12	0.14 (0.46)
13	0.41 (0.27)
14	0.61 (0.17)
15	0.61 (0.17)
16	0.35 (0.30)
23	0.02* (0.68)
24	0.03* (0.65)
25	0.02* (0.71)
26	0.05 (0.59)
27	0.07 (0.56)
28	0.17 (0.43)
35	0.09 (0.52)
36	0.02* (0.68)
37	0.04* (0.62)
38	0.07 (0.56)

3.5 Exploratory correlations and research constraints

3.5.1 Correlation analysis between PN and NOx emissions

The elevated PN and reduced NOx emissions observed in China VI HDDTs compared to China V HDDTs raise the question of whether there exists a systematic relationship between these two pollutants, for example, through known combustion and engine control trade-offs. To investigate this possibility under real-world driving conditions, we performed exploratory correlation analyses using Pearson's and Spearman's rank correlation methods on both trip-based and operating mode-based PN and NOx EFs. Analyses were conducted for the full sample of China VI HDDTs (n=21) and for compliant (n=13) and non-compliant (n=8) subgroups, respectively. The detailed statistical outcomes are presented in Table 5 and Table 6.

Table 5. Pearson correlation test results for PN and NOx EFs

Operating Mode	*p*-value (ρ)		
	All HDDTs	compliant HDDTs	non-compliant HDDTs
all	0.049* (0.43)	0.75 (0.10)	0.77 (0.12)
0	0.15 (0.32)	0.26 (-0.33)	0.77 (0.12)
1ᵃ	0.04* (0.45)	0.88 (0.05)	0.39 (0.35)
12	$8\times10^{-5*}$ (0.75)	0.90 (-0.04)	0.02* (0.78)
13	$3\times10^{-6*}$ (0.83)	0.60 (0.16)	$2\times10^{-4*}$ (0.96)
14	$5\times10^{-6*}$ (0.82)	0.98 (-0.008)	$1\times10^{-3*}$ (0.92)
15	$6\times10^{-5*}$ (0.76)	0.91 (0.04)	0.02* (0.79)
16	0.02* (0.50)	0.79 (0.08)	0.13 (0.58)
22	0.91 (-0.03)	$6\times10^{-3*}$ (0.77)	0.41 (0.34)
23	0.16 (0.32)	0.14 (0.43)	0.86 (0.08)
24	0.20 (0.29)	0.46 (0.22)	0.96 (-0.02)
25	$4\times10^{-4*}$ (0.70)	0.57 (0.17)	$2\times10^{-3*}$ (0.91)
26	0.12 (0.35)	0.85 (0.06)	0.98 (-0.01)
27	0.20 (0.29)	1.00 (-0.0008)	0.95 (0.03)
28	0.12 (0.35)	0.88 (0.04)	0.88 (0.06)
35	0.15 (0.33)	0.95 (-0.02)	0.74 (0.14)
36	0.11 (0.36)	0.73 (-0.11)	0.77 (0.12)
37	0.01* (0.54)	0.69 (-0.12)	0.38 (0.36)
38	0.09 (0.38)	0.50 (-0.20)	0.63 (0.20)

Table 6. Spearman's rank test results for PN and NOx EFs

Operating Mode	*p*-value		
	All HDDTs	compliant HDDTs	non-compliant HDDTs
all	0.02*	0.72	0.74
0	0.54	0.57	1.0
1ᵃ	0.94	0.48	1.0
12	0.02*	0.69	$4\times10^{-3*}$
13	0.24	0.69	0.32
14	0.15	0.93	0.14
15	0.09	0.62	0.12
16	0.20	0.36	0.61
22	0.42	0.61	0.65
23	$6\times10^{-3*}$	0.51	0.35
24	0.02*	0.38	0.82
25	0.046*	0.68	0.04*
26	$8\times10^{-3*}$	0.54	0.96
27	0.08	0.99	0.91
28	0.12	0.83	0.82
35	0.12	0.82	0.96
36	0.11	0.76	1.0

37	0.049*	0.99	0.57
38	0.10	0.97	0.69

For the entire China VI HDDT fleet, a weak positive and monotonic association was found between PN and NOx emissions (Pearson correlation coefficient $\rho=0.43$, $p=0.049$; Spearman $p=0.02$). Statistically significant positive correlations were also identified in several operating modes by the Pearson test (i.e., modes 1, 12-16, 25, and 37, mainly representing low-speed modes) and by the Spearman's test (i.e., modes 12, 23-26, and 37, primarily medium-speed modes). However, these relationships were not consistent across all operating modes, and a majority of mode-specific results were statistically non-significant. For compliant HDDTs, no significant PN-NOx correlations were identified (with the exception for mode 22), while the non-compliant subgroup exhibited several moderate positive correlations (notably in modes 12-15 and 25). The absence of consistent correlation patterns likely reflects the decoupling effect of the after-treatment systems such as DPF and SCR, which regulate PN and NOx emissions via independent pathways. Therefore, further investigations beyond the conventional PN-NOx trade-off framework are needed to identify the underlying causes of the elevated PN emissions observed in China VI HDDTs and to develop effective mitigation strategies.

3.5.2 Research constraints

It should be acknowledged that the dataset used in this research was relatively limited and unbalanced, consisting of 3 China V and 21 China VI HDDTs. This reflects the practical constraints associated with real-world on-road PEMS testing, particularly for China V vehicles, for which such measurements are relatively scarce due to the absence of regulatory requirements and the high cost of testing. Under these conditions, the MWU test was employed as a nonparametric approach appropriate for small and unbalanced sample sizes, provided that observations are independent. Exact inference methods were used to ensure the validity of statistical results without relying on large-sample assumptions. While the limited sample size of the China V group may reduce statistical power and affect the sensitivity to detect subtle differences, statistically significant results obtained under these conditions can be considered indicative of relatively pronounced differences between groups. In contrast, non-significant results should be interpreted with caution and are not taken as evidence of equivalence. In addition, the dataset reflects real-world operating conditions, including variability in driving environments and vehicle usage. Rather than representing strictly controlled experimental comparisons, the analysis aims to capture practical emission behavior under representative conditions. When combined with appropriate statistical methods and careful interpretation, the results provide meaningful insights into emission characteristics and the potential impacts of the transition from China V to China VI standards.

4 Conclusions and future work

This research measured and evaluated the PN and NOx emissions of 24 HDDTs certified under either the China V or China VI emission standards, using on-road PEMS tests conducted in Shenzhen, China. All measurements were performed in accordance with the China VI emission standard GB 17691-2018 (MEE and SAMR, 2018). By aligning the experimental design, test implementation, and data validation process with the national regulatory procedures, the on-road evaluations provide a direct empirical linkage between real-world vehicle emissions and the China VI regulatory framework, enabling a practical assessment of the regulation effectiveness under actual driving conditions. The findings offer quantitative evidence to inform future regulatory refinement and enforcement strategies aimed at achieving the intended emission reduction goals of the regulation.

The analytical framework involved a comparison of the overall emissions between the China V and China VI HDDTs, followed by the stratification of China VI HDDTs into compliant and non-compliant groups based on real-world emission compliance. This approach enabled both an evaluation of the China VI standard's overall effectiveness and an investigation of emission disparities linked to compliance status. Subsequent analyses examined emission characteristics across detailed vehicle operating modes to identify potential weaknesses in current emission control strategies. In addition, the performance of the SCR after-treatment systems under different operating conditions was assessed using OBD NOx concentration data to quantify in-use NOx reduction efficiencies. The operating mode-specific effectiveness of EGR systems in controlling NOx emissions was also evaluated to identify future directions for both regulatory and technical improvements.

The results suggest that emission noncompliance among a notable proportion of China VI HDDTs partially undermined the intended benefits of the new standard. Specifically, PN and NOx EFs for China VI non-compliant HDDTs were 1,695.6% and 85.6% higher than those of China V HDDTs, respectively. Although China VI compliant HDDTs achieved mean reductions of 51.5% in PN and 59.6% in NOx relative to China V vehicles, these gains were offset by the extreme emissions of non-compliant vehicles, resulting in net overall reductions of −447.7% (PN) and +25.1% (NOx) for the China VI fleet. These findings highlight the need for strengthened in-use compliance inspection and enforcement mechanisms to ensure emission control effectiveness. Vehicle operating conditions exerted a visible influence on emission behavior. China VI HDDTs generally exhibited higher mean PN emissions than China V HDDTs under most operating modes, in which, non-compliant China VI vehicles showed consistently higher mean emissions across all operating modes, while compliant vehicles still exceeded China V levels in most low-to-medium speed bins. The MWU test also identified the higher PN EFs of non-compliant China VI HDDTs were statistically significant in medium speed bins. In contrast, the mean NOx emissions from China VI HDDTs were generally lower than those from China V HDDTs, with compliant vehicles showing reductions across most operating modes. However, higher mean NOx EFs were observed from non-compliant China VI HDDTs in modes characterized by high vehicle specific power (VSP). Targeted controls for PN and NOx emissions under the identified conditions are therefore needed.

The SCR after-treatment system was found to be indispensable for NOx emission control. It achieved reductions of 76.6-96.8% in NOx concentrations. Without SCR, compliance with the China VI requirement that 95% of NOx concentration data remain below 500 ppm would not be achievable (as depicted in Fig. 4(a)). Nevertheless, the SCR efficiency varied by operating mode and compliance status, with lower reductions under low speed conditions and for non-compliant HDDTs. Correlation analyses revealed that SCR NOx reductions were positively associated with operating mode for compliant HDDTs, possibly due to the increased exhaust temperatures at higher speeds, as confirmed by the Pearson and Spearman's rank correlation tests, which enhanced urea decomposition and catalyst activity. In contrast, no such correlation was detected for non-compliant HDDTs, possibly due to their significantly decreased NOx reductions in high-speed modes, as identified by the MWU test. Consequently, regulatory and technological measures to enhance the SCR functionality in low-speed modes may yield additional NOx mitigation benefits, and in-use compliance monitoring focusing on high-speed modes could help identify non-compliant HDDTs more efficiently. The analysis of the EGR systems confirmed their in-use effectiveness in controlling NOx emissions from China VI HDDTs as well. EGR-equipped vehicles consistently exhibited lower mean NOx EFs than those without EGR across all operating modes, with reductions ranging from 43.5% to 75.7%. The MWU test revealed that NOx EF differences were statistically significant under several medium- and high-speed operating modes for compliant vehicles, reflecting the contribution of EGR to effective NOx mitigation under real-world driving conditions. However, the EGR performance at low speeds requires further investigation and possible optimization.

The findings of this study have important implications for multiple stakeholders. For regulatory authorities, the results provide empirical evidence on the real-world effectiveness of the transition from China V to China VI standards, supporting the evaluation and potential refinement of emission control policies and compliance monitoring strategies. For vehicle manufacturers, the identified differences in emission characteristics and after-treatment system performance offer practical insights into areas where emission control technologies, such as SCR systems, can be further optimized. In addition, the results contribute to a better understanding of real-world emission behavior, which can inform future policy development and technological improvements aimed at achieving more effective emission reductions.

For future work, large-scale field tests with more balanced samples would help improve the robustness of statistical comparisons and enable more comprehensive analyses, such as linking HDDT emissions with continuous vehicle operation profiles. Given the high PN emissions observed in this research, further investigation into PN formation mechanisms, impact factors and mitigation strategies is also recommended. To provide a more detailed quantitative understanding of SCR behavior under dynamic driving conditions and improve predictive capability for emission control, explorations on regression-based or machine-learning models to quantify the relationships among SCR efficiency, vehicle speed, exhaust temperature, and NOx emissions are significant research directions as well. In addition, investigations on regulatory refinement and enforcement strategies can also be valuable directions. For example, the finding that nearly 30% of China VI HDDTs were emission non-compliant underscores the need for practical regulatory responses, e.g., strengthening periodic in-use inspections, expanding PEMS-based compliance testing, or deploying remote sensing technology, are needed. Although the current China VI standard mandates OBD-based NOx reporting, it does not provide sufficient information to fully assess the in-use performance of SCR systems. Requiring the reporting of both upstream and downstream NOx concentrations could support direct assessment of SCR efficiency under real-world conditions. Integrating such OBD data with predictive or machine-learning models could also enhance regulatory oversight and enable data-driven compliance management. In addition, establishing remote PN monitoring analogous to NOx reporting, and promoting big-data driven and online compliance evaluation to identify potential high emitters for targeted PEMS inspections, may also help ensure the intended environmental benefits of the China VI standard.

CRediT authorship contribution statement

Weixia Li: Conceptualization, Formal analysis, Methodology, Software, Visualization, Writing - original draft. **Ling Miao**: Data curation, Investigation, Validation, Writing - review & editing. **Guoyuan Wu**: Formal analysis, Methodology, Writing - review & editing. **Wenwei Huang**: Project administration, Resources, Supervision, Conceptualization, Writing - review & editing. **Yi Zhang**: Supervision, Formal analysis, Writing - review & editing.

Replication and data sharing

The dataset and code used in this research is partially available at https://doi.org/10.26599/ETSD.2026.9190018.

Acknowledgements

This research was funded by Shenzhen Polytechnic University Research Fund (grant number: 6024310009K) and Research Project of Department of Education of Guangdong Province (grant number: 2023ZDZX3078).

Declaration of competing interest

The authors declare that they have no known competing financial interests or personal relationships that could have appeared to influence the work reported in this paper.

References

Ministry of Ecology and Environment of the People's Republic of China (MEE), 2026. China Mobile Source Environmental Management Annual Report, 2025. Available at: https://www.mee.gov.cn/hjzl/sthjzk/ydyhjgl/202512/W020251203577003736659.pdf (accessed on May 20, 2026) (in Chinese)

United States Environmental Protection Agency (USEPA), 2025. Transportation Sector Emissions. Available at: https://www.epa.gov/ghgemissions/transportation-sector-emissions (accessed on November 15, 2025).

United States Environmental Protection Agency (USEPA), 2023. Smog, Soot, and Other Air Pollution from Transportation. Available at: https://www.epa.gov/transportation-air-pollution-and-climate-change/smog-soot-and-other-air-pollution-transportation (accessed on November 15, 2025)

California Air Resources Board (CARB), 2020. Public hearing to consider the proposed heavy-duty engine and vehicle omnibus regulation and associated amendments. Available at: https://ww3.arb.ca.gov/regact/2020/hdomnibuslownox/isor.pdf (accessed on November 15, 2025)

EMISA, 2023. European Road Transport & Emissions (ERTE) Trends Report 2023. Available at: https://erte.report/ertefiles/ERTE2023_Complete_Downloable.pdf (accessed on November 15, 2025)

Zhang, B., Cheng, S., Lu, F., Lei, M., 2022. Estimation of exposure and premature mortality from near-roadway fine particulate matter concentrations emitted by heavy-duty diesel trucks in Beijing, Environmental Pollution. 311, 119990. https://doi.org/10.1016/j.envpol.2022.119990

State Energy and Environment Impact Center (SEEIC), 2022. Environmental Justice, NYU Law. Available at: https://www.law.nyu.edu/centers/state-impact/projectsreports/projects/climate-and-health/environmental-justice (accessed on November 15, 2025)

European Environment Agency (EEA), 2022. Health impacts of air pollution in Europe. Available at: https://www.eea.europa.eu/publications/air-quality-in-europe-2022/health-impacts-of-air-pollution (accessed on November 15, 2025)

European Environment Agency (EEA), 2024. Europe's air quality status 2024. Available at: https://www.eea.europa.eu//publications/europes-air-quality-status-2024 (accessed on November 15, 2025)

California Air Resources Board (CARB), 2021. Advanced Clean Fleets Regulation Summary: Accelerating Zero-Emission Truck Markets. Available at: https://ww2.arb.ca.gov/sites/default/files/2021-08/210817acffactsheet.pdf (accessed on November 15, 2025)

European Union, 2024. Regulation (EU) 2024/1527 of the European parliament and of the council. Available at: https://eur-lex.europa.eu/legal-content/EN/TXT/PDF/?uri=OJ:L_202401257 (accessed on November 15, 2025)

Ministry of Ecology and Environment (MEE) and State Administration for Market Regulation (SAMR) of the People's Republic of China, 2018. Limits and measurement methods for emissions from diesel fuelled heavy-duty vehicles (China VI). Available at: https://www.mee.gov.cn/ywgz/fgbz/bz/bzwb/dqhjbh/dqydywrwpfbz/201807/W020180703397013304274.pdf (accessed on November 15, 2025) (in Chinese).

Papadopoulos, G., Ntziachristos, L., Tziourtzioumis, C., Keramydas, C., Lo, T.-S., Ng, K.-L., Wong, H.-L.A., Wong, C.K.-L., 2020. Real-world gaseous and particulate emissions from Euro IV to VI medium duty diesel trucks, Science of the Total Environment, 731, 139137. https://doi.org/10.1016/j.scitotenv.2020.139137

He, L., Zhang, S., Hu, J., Li, Z., Zheng, X., Cao, Y., Xu, G., Yan, M., Wu, Y., 2020. On-road emission measurements of reactive nitrogen compounds from heavy-duty diesel trucks in China, Environmental Pollution, 262, 114280. https://doi.org/10.1016/j.envpol.2020.114280

Shen, X., Lv, T., Zhang, X., Cao, X., Li, X., Wu, B., Yao, X., Shi, Y., Zhou, Q., Chen, X., 2021. Real-world emission characteristics of black carbon emitted by on-road China IV and China V diesel trucks, Science of The Total Environment, 799, 149435. https://doi.org/10.1016/j.scitotenv.2021.149435

Wu, B., Xuan, K., Zhang, X., Wu, Z., Wang, W., Shen, X., Li, X., Zhang, H., Cao, X., Hao, X., 2022. Quantitative of instantaneous BC emissions based on vehicle specific power from real-world driving diesel trucks in China, Science of the Total environment, 819, 153230. https://doi.org/10.1016/j.scitotenv.2022.153230

Zhang, Y., Song, Y., Feng, T., Chen, Y., 2023. Comparative Analysis of Emission Characteristics of In-Use China II–V Gasoline, Hybrid, Diesel-Fueled Vehicles, Atmosphere, 14, 272. https://doi.org/10.3390/atmos14020272

Zhao, H., He, H., Lu, D., Zhou, D., Lu, C., Fang, X., Peng, Z., 2024. Evaluation of CO2 and NOx emissions from container diesel trucks using a portable emissions measurement system, Building and Environment, 252, 111266. https://doi.org/10.1016/j.buildenv.2024.111266

Li, P., Lü, L., 2021. Evaluating the real-world NOx emission from a China VI heavy-duty diesel vehicle, Applied Sciences, 11, 1335. https://doi.org/10.3390/app11031335

Wang, J., Wang, R., Yin, H., Wang, Y., Wang, H., He, C., Liang, J., He, D., Yin, H., He, K., 2022. Assessing heavy-duty vehicles (HDVs) on-road NOx emission in China from on-board diagnostics (OBD) remote report data, Science of The Total Environment, 846, 157209. https://doi.org/10.1016/j.scitotenv.2022.157209

Hao, L., Ren, Y., Lu, W., Jiang, N., Ge, Y., Wang, Y.J.A., 2023. Assessment of heavy-duty diesel vehicle NOx and CO2 emissions based on OBD data, Atmosphere, 14, 1417. https://doi.org/10.3390/atmos14091417

Ge, Y., Hou, P., Lyu, T., Lai, Y., Su, S., Luo, W., He, M., Xiao, L., 2023. Machine learning-aided remote monitoring of NOx emissions from heavy-duty diesel vehicles based on OBD data streams, Atmosphere, 14, 651. https://doi.org/10.3390/atmos14040651

Li, X., Ai, Y., Ge, Y., Qi, J., Feng, Q., Hu, J., Porter, W.C., Miao, Y., Mao, H., Jin, T., 2022. Integrated effects of SCR, velocity, and Air-fuel Ratio on gaseous pollutants and CO2 emissions from China V and VI heavy-duty diesel vehicles, Science of the Total Environment, 811, 152311. https://doi.org/10.1016/j.scitotenv.2021.152311

Ge, Z., Li, W., Wang, J., Wang, Y., Huang, Y., Wang, X., Ge, Y., 2025. Real-road NOx and CO2 emissions of city and highway China-6 heavy-duty diesel vehicles, Journal of Environmental Sciences, 149, 330-341. https://doi.org/10.1016/j.jes.2023.11.018

He, L., Li, G., Wu, X., Zhang, S., Tian, M., Li, Z., Huang, C., Hu, Q., Wu, Y., Hao, J., 2024. Characteristics of NOx and NH3 emissions from in-use heavy-duty diesel vehicles with various aftertreatment technologies in China, Journal of Hazardous Materials, 465, 133073. https://doi.org/10.1016/j.jhazmat.2023.133073

Tian, M., He, L., Peng, D., Fu, M., Ma, S., Mu, J., Yu, Q., Wang, J., Yin, H., Wang, J., 2024. Characterizing NOx emissions from diesel trucks with tampered aftertreatment systems and its implications for identifying high emitters, Science of the Total Environment, 917, 170378. https://doi.org/10.1016/j.scitotenv.2024.170378

Li, W., Dong, Z., Miao, L., Wu, G., Deng, Z., Zhao, J., Huang, W., 2024. On-road evaluation and regulatory recommendations for NOx and particle number emissions of China VI heavy-duty diesel trucks: A case study in Shenzhen, Science of The Total Environment, 928, 172427. https://doi.org/10.1016/j.scitotenv.2024.172427

Ayodhya, A.S., Narayanappa, K.G., 2018. An overview of after-treatment systems for diesel engines, Environmental Science and Pollution Research, 25, 35034-35047. https://doi.org/10.1007/s11356-018-3487-8

Sensors Inc., 2025a. SEMTECH ECOSTAR PLUS Mobile Test System for On-Road and Non-Road Applications. Available at: https://d3pcsg2wjq9izr.cloudfront.net/files/28865/download/415639/5-SEMTECH_ECOSTAR_Plus.pdf (Accessed on November 16, 2025)

Sensors Inc., 2025b. Particle number measurement SEMTECH CPN. Available at: https://sensors-inc.com/Products/SEMTECH/CPN (Accessed on November 16, 2025)

Merkisz, J., Lijewski, P., Fuć, P., Rymaniak, Ł., Ziółkowski, A., 2017. Measurement of exhaust emissions under actual operating conditions with the use of PEMS: Review of selected vehicles, IntechOpen. DOI: 10.5772/intechopen.70442

Koupal, J., Landman, L., Nam, E., Warila, J., Scarbro, C., Glover, E., Giannelli, R., 2005. MOVES2004 Energy and Emission Inputs Draft Report, U.S. Environmental Protection Agency, Report No. EPA420-P-05-003. Available at:

https://nepis.epa.gov/Exe/ZyPDF.cgi/P1001DAQ.PDF?Dockey=P1001DAQ.PDF

U.S. Environmental Protection Agency (EPA), 2009. Development of emission rates for heavy-duty vehicles in the Motor Vehicle Emissions Simulator (Draft MOVES2009), Report No. EPA-420-P-09-005, Washington DC, USA. Available at: https://nepis.epa.gov/Exe/ZyPDF.cgi/P100F80L.PDF?Dockey=P100F80L.PDF

Wu, Y., Zhang, S., Li, M., Ge, Y., Shu, J., Zhou, Y., Xu, Y., Hu, J., Liu, H., Fu, L., 2012. The challenge to NO x emission control for heavy-duty diesel vehicles in China, Atmospheric Chemistry and Physics, 12, 9365-9379. https://doi.org/10.5194/acp-12-9365-2012

Zheng, X., Wu, Y., Jiang, J., Zhang, S., Liu, H., Song, S., Li, Z., Fan, X., Fu, L., Hao, J., 2015. Characteristics of on-road diesel vehicles: black carbon emissions in Chinese cities based on portable emissions measurement, Environmental science & technology, 49, 13492-13500. https://doi.org/10.1021/acs.est.5b04129

Jimenez-Palacios, J.L., 1998. Understanding and quantifying motor vehicle emissions with vehicle specific power and TILDAS remote sensing, Massachusetts Institute of Technology. Available at: http://hdl.handle.net/1721.1/44505

Mann, H.B. and Whitney, D.R., 1947. On a test of whether one of two random variables is stochastically larger than the other. The annals of mathematical statistics, pp.50-60. https://www.jstor.org/stable/2236101

Fay, M.P. and Proschan, M.A., 2010. Wilcoxon-Mann-Whitney or t-test? On assumptions for hypothesis tests and multiple interpretations of decision rules. Statistics surveys, 4, p.1. https://doi.org/10.1214/09-SS051

Kerby, D.S., 2014. The simple difference formula: An approach to teaching nonparametric correlation. Comprehensive Psychology, 3, pp.11-IT. https://doi.org/10.2466/11.IT.3.1

Benesty, J., Chen, J., Huang, Y. and Cohen, I., 2009. Pearson correlation coefficient. In Noise reduction in speech processing (pp. 1-4). Berlin, Heidelberg: Springer Berlin Heidelberg. https://doi.org/10.1007/978-3-642-00296-0_5

Conover, W.J., 1999. Practical nonparametric statistics. john wiley & sons.

Tan, L., Guo, Y., Liu, Z., Feng, P., Li, Z., 2019. An investigation on the catalytic characteristic of NOx reduction in SCR systems, Journal of the Taiwan Institute of Chemical Engineers, 99, 53-59. https://doi.org/10.1016/j.jtice.2019.02.020

Deng, B., Cai, W., Zhang, W., Bian, L., Che, X., Xiang, Y., Wu, D., 2025. A comprehensive investigation of EGR (exhaust gas recirculation) effects on energy distribution and emissions of a turbo-charging diesel engine under World Harmonized transient cycle, Energy, 316, 134506. https://doi.org/10.1016/j.energy.2025.134506

Author biography

Weixia LI received her Ph.D degree from Tsinghua University in 2017. From 2015 to 2016, she conducted her research at the University of California, Riverside as a visiting research student. She worked as a Postdoctoral Researcher at Tsinghua University from 2017 to 2019 and now is a Lecturer at Shenzhen Polytechnic University. Her major research interests include intelligent connected vehicle technologies, vehicle energy/emissions modeling, eco-routing, and eco-driving.

Ling MIAO received his MS degree from Shandong University in 2015. Currently he is a research engineer at Shenzhen Polytechnic University. His research interests focus on motor vehicle emission control and management.

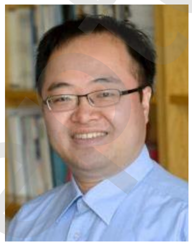

Guoyuan WU received his Ph.D. degree from UC Berkeley in 2010. He worked as a Postdoctoral Fellow, Assistant Research Faculty and Associate Research Faculty UC Riverside, in 2010, 2012 and 2018, respectively. Since July 2022, Dr. Wu has been working as a Full Research Faculty. In addition, he has been holding an Adjunct Professorship at UC Riverside since 2017. His research interests include development and evaluation of sustainable and intelligent transportation systems, optimization and control of transportation systems, traffic flow modeling and simulation, and vehicle emissions and powertrain modeling.

Wenwei HUANG received his Ph.D degree from Beijing Jiaotong University in 2019. He is currently a professor at Shenzhen Polytechnic University. His research interests focus on motor vehicle emission analyses and pollutants control technology.

Yi ZHANG received his PhD degree from the University of Strathclyde, UK in 1995. He is currently a professor in control science and engineering at Tsinghua University. His current research interests focus on intelligent transportation systems. His active research areas include intelligent vehicle-infrastructure cooperative systems, analysis of urban transportation systems, urban road network management, traffic data fusion and dissemination, and urban traffic control and management. His research fields also cover the advanced control theory and applications, advanced detection and measurement, and systems engineering.